Int. J. Mach. Tools Manufact. Vol. 31, No. 2, pp.167–181, 1991.
Printed in Great Britain

0890–6955/91$3.00 + .00
Pergamon Press plc

GENERATION AND GEOMETRY OF HYPOID GEAR-MEMBER WITH FACE-HOBBED TEETH OF UNIFORM DEPTH

F. L. LITVIN,* W. S. CHAING,* C. KUAN,* M. LUNDY† and W. J. TSUNG†

(*Received* 23 *August* 1989; *in final form* 15 *August* 1990)

Abstract—The authors have described the method and kinematics for generation of hypoid gear-members with face-hobbed teeth of uniform depth and derived equations for the tool geometry and the tooth surface. The developed equations are necessary for the computerized inspection of gear tooth surface by coordinate measuring machines, for generation of dies to forge the gears, and to represent partially the input data for computerized simulation of meshing and contact of hypoid gear drives.

1. INTRODUCTION

HYPOID gears have found widespread application in the automotive industry. They are manufactured using cutting machines designed by the Gleason Work (U.S.A.) and Oerlikon (Switzerland).

A hypoid gear drive is designed for transformation of motions between crossed axes. The reference surfaces of the pinion and gear are pitch cones that are in tangency at point P (pitch point) chosen in the fixed coordinate system (Fig. 1). Usually, the axes of rotation of hypoid gears form an angle of 90°. The shortest distance between the axes of rotation is designated by E and the apices of pitch cones are notified by O_1 and O_2. The plane that is tangent to the pitch cones (pitch plane) passes through the apices of the pitch cones and pitch point P. Figure 2 shows pitch point P, the shortest distance E, the angular velocities $\boldsymbol{\omega}^{(1)}$ and $\boldsymbol{\omega}^{(2)}$ of the pinion and the gear; d_1 and d_2 determine the location of apices of pitch cones O_1 and O_2 with respect to gear shortest distance.

There are two types of hypoid gears: (i) with tapered teeth, and (ii) with teeth of uniform depth, and they are generated respectively by: (i) the face-milled method, and (ii) the face-hobbed one.

The face-milled method is based on the application of a tool whose generating surface is a cone. The teeth are tapered. Each tooth (sometimes even each side of the tooth) is generated separately and indexing is required for the generation of the next tooth. The gear tooth surface is an envelope of the family of tool surfaces. The exception is the formate-cut gear whose surface coincides with the tool surface.

The face-hobbed method is based on generation of the tooth surface by two finishing blades. The tooth surface represents a family of curves (straight lines) that is generated by the shape of the blade. The teeth are of uniform depth. The process for generation is a continuous one and indexing is not required.

The theory of generation and mathematical description of hypoid gears with tapered tooth surfaces has been the subject of intensive research by Gleason engineers [1], and Litvin *et al.* [2]. Methods for determination of an envelope of a family of surfaces have been discussed by Litvin [3].

The theory of generation and mathematical representation of surfaces for face-hobbed hypoid gears has not been published in the literature.

There are several reasons why mathematical representation of hypoid gear tooth surfaces is important for manufacturing them with high precision:

*Department of Mechanical Engineering, University of Illinois at Chicago, Illinois, U.S.A.
†Gear Engineering Department, Dana Corporation, Indiana, U.S.A.

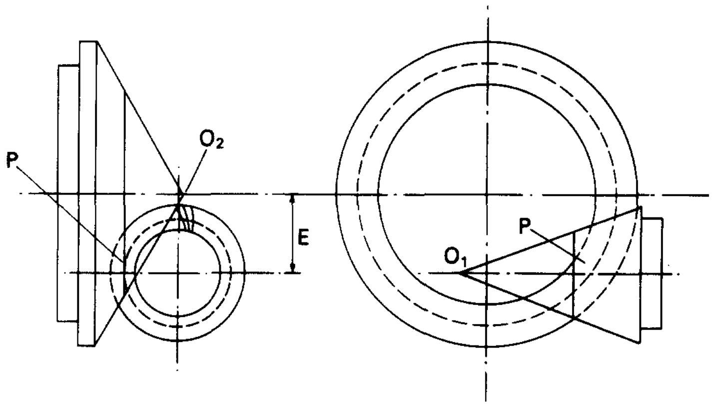

FIG. 1. Pitch cones of hypoid gears.

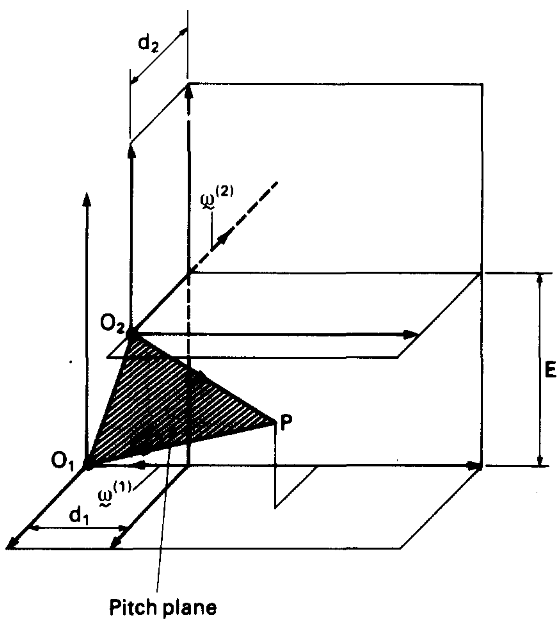

FIG. 2. Pitch plane of hypoid gears.

(1) It is necessary to optimize the machine-tool settings in order to reduce the level of transmission errors (they cause vibrations) and provide a proper bearing contact. This can be achieved by computerized simulation of meshing and contact of gear tooth surfaces in continuous tangency. Analytically, this means that the gear tooth surfaces must have a common position vector and collinear normal at any instantaneous point of contact [3].

(2) It is necessary to compensate for the distortion of gear tooth surfaces that are caused by heat-treatment and by errors in the installment of machine-tool settings. This goal can be achieved by proper corrections of machine-tool settings. For this purpose the tooth surface of the first gear from the set of gears to be generated is inspected by a coordinate measuring machine [2, 4, 5]. This inspection provides the information on deviations of the real tooth surfaces from the theoretical one that must be represented analytically. The minimization of deviations by correction of a limited number parameters—the machine-tool settings—is a typical mathematical problem of optimization.

(3) Forging of gears requires generation of dies that have to copy the gear tooth surfaces. The dies are generated point by point and this can be done if the gear tooth surface is represented analytically.

The three reasons above explain why analytical representation of face-hobbed gear tooth surfaces will benefit their manufacturing. The contents of this paper cover the description of the method for generation of the gear-member of face-hobbed gear drives, and the analytical representation of the gear tooth surface. The obtained results are the basis for: (i) determination of tooth surface deviations by coordinate measurements, (ii) generation of dies for forging, and (iii) as part of the input data for computerized simulation meshing and contact of hypoid gear drives [2, 6].

2. PRINCIPLES OF GEAR TOOTH SURFACE GENERATION

The principle of gear tooth generation is shown schematically in Fig. 3. The head cutter is provided with N_w groups of blades. Each group contains 3 blades: one for rough cutting and two finishing blades—one for each side of the tooth. While the head cutter is rotated through the angle $2\pi/N_w$, the being generated gear is rotated through the angle $2\pi/N_2$, where N_2 is the number of gear teeth. Thus the next group of blades will start to cut the next gear tooth after the current group of blades has finished cutting the current tooth. The transmission of the cutting machine provides related rotations of the head cutter and the gear and this is the condition of the continuous indexing.

The schematic of the cutting machine is shown in Fig. 4. The machine cradle carries the head cutter. The axis of the gear blank forms with the axis of the cradle the prescribed angle that depends on the pitch cone angle of the gear. In the process for generation the cradle, the head cutter and the gear perform related rotations about their axes.

The instalment of the head cutter and the gear on the cutting machine are shown in Fig. 5. S_{c2} is the coordinate system that is rigidly connected to the cutting machine. An auxiliary coordinate system S_r is also rigidly connected to the cutting machine. Plane $x_{c2} = 0$ is the so-called machine plane and the origin O_{c2} of S_{c2} is the machine center.

We will differentiate betwen nontilted and tilted settings of the head cutter (Figs 3 and 5). If the head cutter is not tilted, its axis with unit vector **c** coincides with the axis of rotation x_r (Fig. 5). The tilt angle of the head cutter is designated μ_2 (Fig. 5). The tilt of the head cutter is used to improve the conditions of gear meshing and bearing

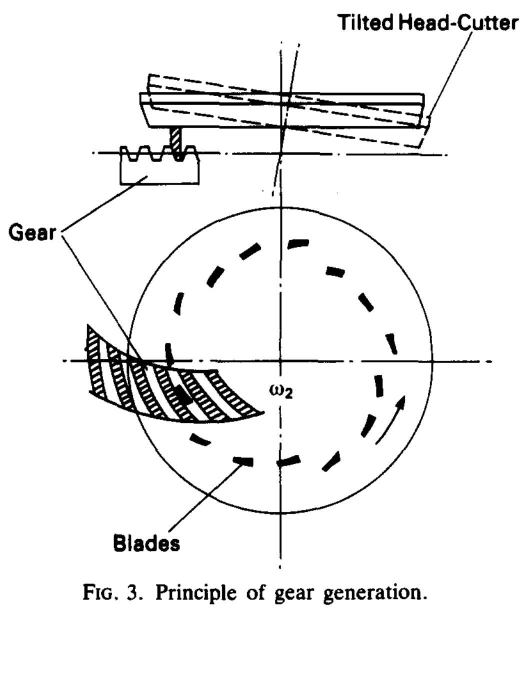

FIG. 3. Principle of gear generation.

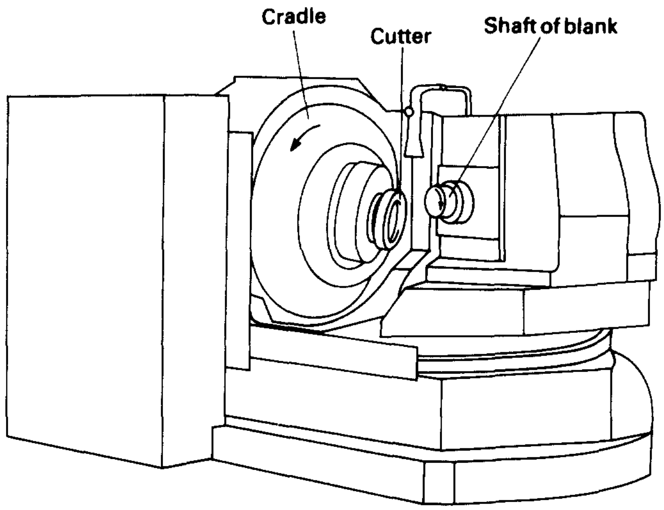

FIG. 4. Schematic of cutting machine.

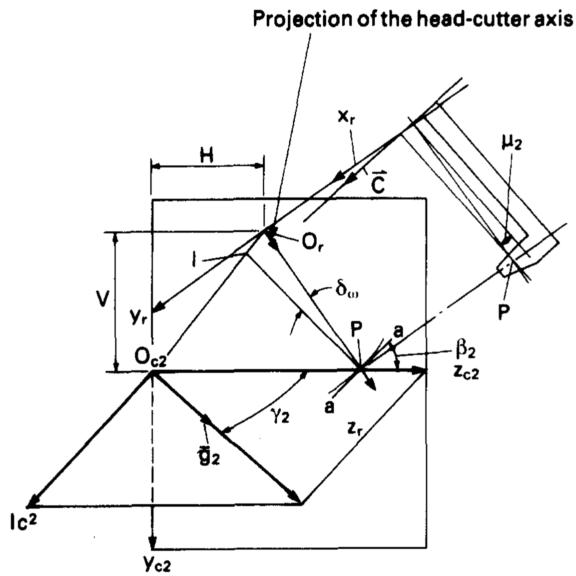

FIG. 5. Cutting machine coordinate system.

contact. The origin O_r of S_r is the point of intersection of the axis of rotation of the head cutter with the machine plane. Parameters V and H represent the coordinates of O_r in the machine plane. The determination of V and H will be discussed below. Point P that lies on the z_{c2}-axis is the pitch point—the point of tangency of the pitch cones.

The axis of the gear blank is located in plane $y_{c2} = 0$ and forms angle γ_2 with the z_{c2}-axis (Fig. 5). Here γ_2 is the gear pitch cone angle, and $\mathbf{g}_2$ is the unit vector of gear axis. While the head cutter rotates about x_r, the gear rotates about g_2. Axis x_{c2} is the cradle rotation axis, but in the process of generation of the gear-member, the cradle of the cutting machine is held at rest.

Parameter β_2 that is shown in Fig. 5 determines the gear "spiral" angle at P and is formed between line a–a and the z_{c2}-axis. Line a–a is perpendicular to PI, and PI and PO_r form an angle δ_w. The blades of the head cutter lie in a plane that passes through PI and is parallel to axis x_r.

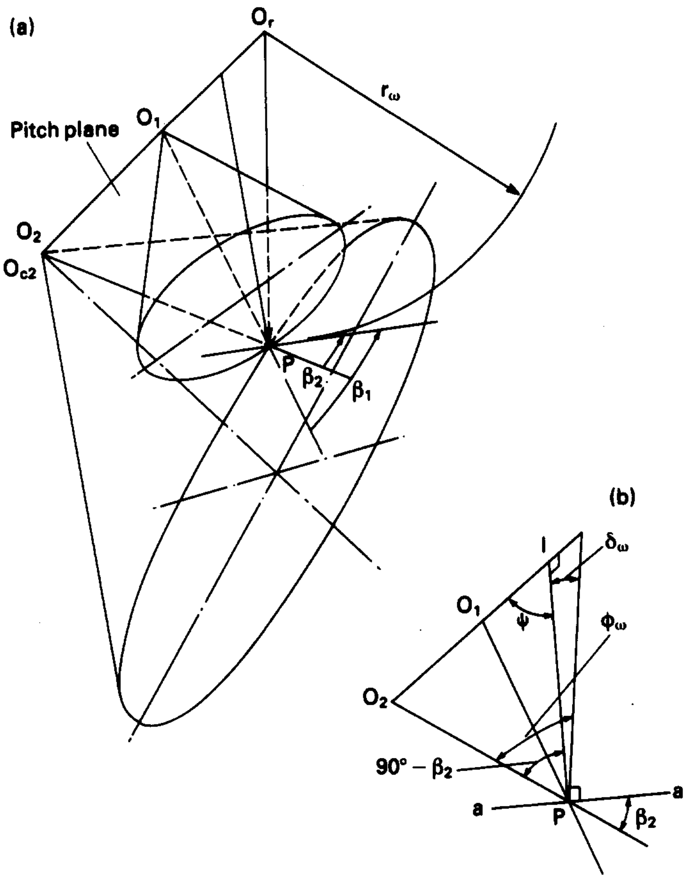

FIG. 6. Instalment of head cutter in pitch plane.

We may also identify the machine plane $x_{c2} = 0$ (Fig. 5) as the pitch plane that is tangent to the pinion and gear pitch cones at the pitch point P (Fig. 6a). The axis of the head cutter, if not tilted, passes through point O_r and is perpendicular to the pitch plane.

The derivation of angle δ_w that is one of the instalment parameters is based on following considerations: We may consider that I is the instantaneous center of rotation, while the head cutter rotates about O_r and an imaginary crown-gear rotates about O_2. Then we obtain (Fig. 6) that

$$\frac{O_rI}{O_2I} = \frac{N_w}{N_{cg}} = \frac{N_w}{\dfrac{N_2}{\sin \gamma_2}} . \tag{1}$$

Here: N_w is the number of head cutter blade groups; N_{cg} is the number of teeth of the imaginary crown gear; N_2 and γ_2 are the number of teeth and the pitch cone angle of the member-gear.

The drawings of Fig. 6(b) yield

$$O_2I = O_2P \frac{\sin(90° - \beta_2)}{\sin \psi} = \frac{r_2}{\sin \gamma_2} \frac{\cos \beta_2}{\sin \psi} \tag{2}$$

$$O_rI = O_rP \frac{\sin \delta_w}{\sin(180° - \psi)} = r_w \frac{\sin \delta_w}{\sin \psi} . \tag{3}$$

Here: r_2 is the radius of gear pitch cone at P and r_w is the head cutter radius. Equations (1) and (3) yield

$$\sin \delta_w = \frac{N_w r_2 \cos \beta_2}{N_2 r_w}. \tag{4}$$

Figure 6(a) shows the instalment parameter ϕ_w that is the so called swivel angle. The drawings of Fig. 6(b) yield that

$$\phi_w = 90° - \beta_2 + \delta_w. \tag{5}$$

3. TOOL GEOMETRY

As it was mentioned above, the tool is provided with groups of blades, and each group contains two finishing blades and one blade for rough cutting (Fig. 3). The following discussions are limited to the geometry of finishing blades.

Figure 7 shows a coordinate system S_c that is rigidly connected to the head cutter. The shape of the inside blade edge is a straight line or a curve that lies in plane II. This plane forms angle δ_w with the plane $y_c = 0$. Both sides of the tooth are generated separately, and each finishing blade is provided with a single edge. The shape of the outer edge of the blade is represented by a dashed line. We designate with r_w the distance between the blade axis of symmetry with the head cutter axis x_c.

Figure 8 shows the location of two finishing blades in coordinate system S_c. The magnitude of angle Ω, that determines the angular location of an outside blade edge with respect to the inside blade edge, depends on the applied number of groups and is determined with

$$\Omega = \frac{2\pi}{N_w} \tag{6}$$

where N_w is the number of applied blade groups. Henceforth, we will consider that $\Omega = 0$ in order to simplify the following derivations.

We consider two auxiliary coordinate systems S_l and S_p that are also rigidly connected to the blade and head cutter (Fig. 8). Axes x_l and x_p coincide each with other and with the axis of symmetry of a two-sided blade. Henceforth, we will consider two cases: (i) straight-lined blade edges, and (ii) curve-lined blade edges. The application of curve-lined blades allows to control the shape and dimensions of the bearing contact.

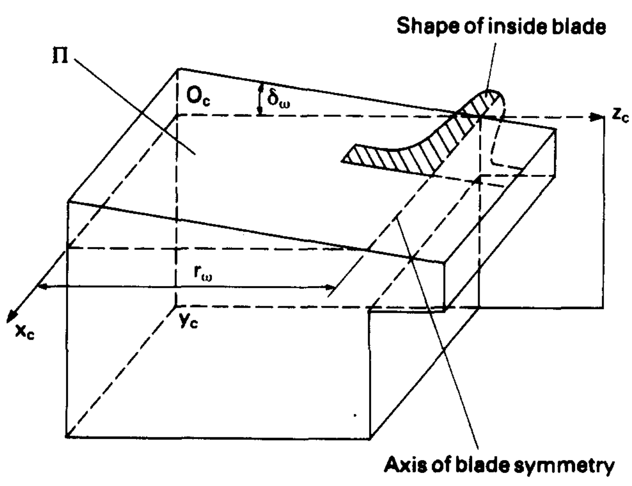

FIG. 7. Blade instalment in S_c.

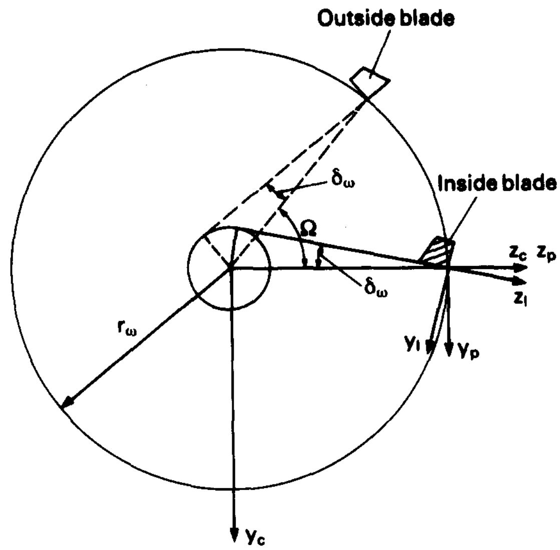

FIG. 8. Instalment of finishing blades.

Blade with straight-lined edges

Figure 9(a) shows a straight-lined blade. It is not excluded that edge angles α_1 and α_2 are of different magnitudes. A position vector $\overline{O_1N_i}$ of a current point N_i of the blade is represented by vector-equation

$$\overline{O_1N_i} = \overline{O_1M_i} + \overline{M_iN_i}. \qquad (i = 1,2) \tag{7}$$

Here $|\overline{M_iN_i} = u_i$. A negative sign for u corresponds to the case where the sense of vector $\overline{M_iN_i}$ is opposite to that shown in Fig. 9(a). Equation (7) yields

$$\mathbf{r}_1(u) = \begin{bmatrix} a_i \cos\alpha_i \sin\alpha_i + u_i \cos\alpha_i \\ 0 \\ \mp a_i \cos^2\alpha_i \pm u_i \sin\alpha_i \end{bmatrix}. \tag{8}$$

Here, a_i is the blade width in the pitch plane; α_i is the blade angle; the upper sign corresponds to point N_1 and the lower sign to point N_2.

Curve blade (Fig. 9b)

The curve is an arc of a circle centered at C_i that lies on the extended line $\overline{O_iM_i}$ (Fig. 9b). The position vector $\overline{O_1N_i}$ of current point N_i is represented by vector equation

$$\overline{O_1N_i} = \overline{O_1C_i} + \overline{C_iN_i}. \tag{9}$$

Here

$$\overline{O_1C_i} = (\rho_i + a_i \cos\alpha_i)\,[\sin\alpha_i \quad 0 \quad \mp \cos\alpha_i]^{\mathrm{T}} \tag{10}$$

$$\overline{C_iN_i} = \rho_i \left[\sin\left(\alpha_i - \frac{u_i}{\rho_i}\right) \quad 0 \quad \pm \cos\left(\alpha_i - \frac{u_i}{\rho_i}\right) \right]^{\mathrm{T}} \tag{11}$$

where u_i is the curvilinear coordinate of the curve. Equations (9)–(11) yield the following equations of the curved blade

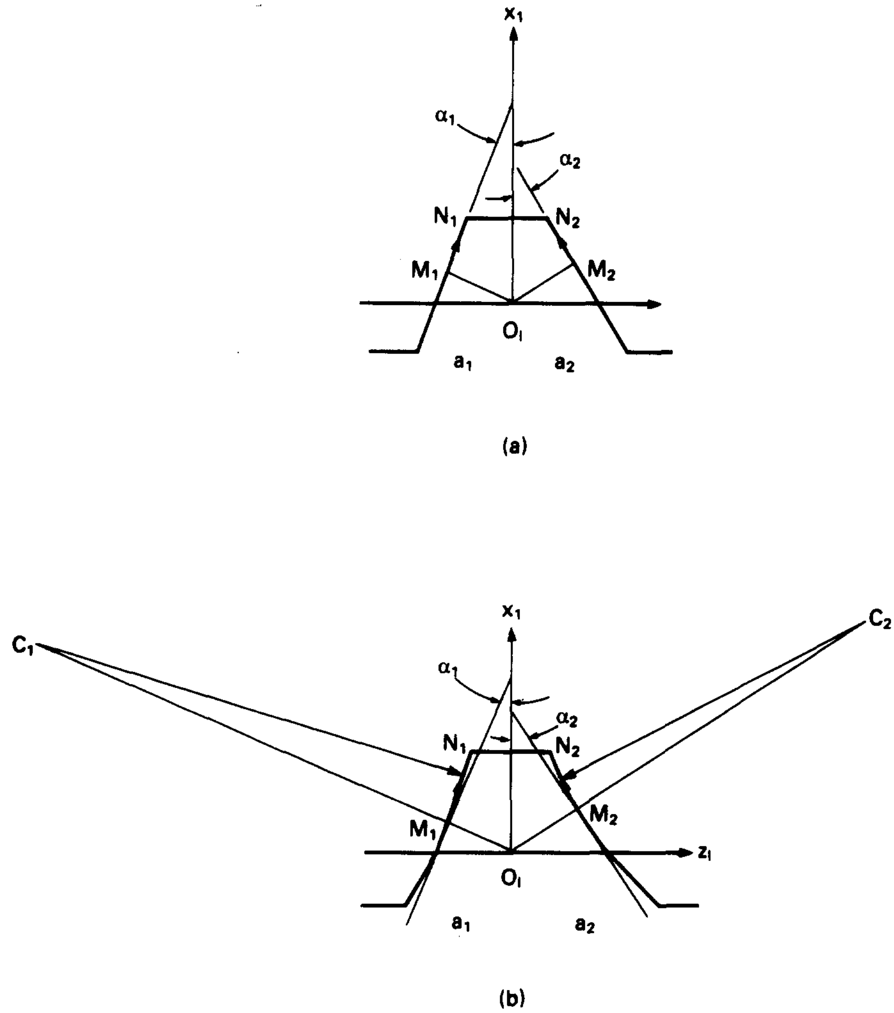

FIG. 9. Member gear cutter blades.

$$\mathbf{r}_l(u_i) = \begin{bmatrix} (\rho_i + a_i \cos\alpha_i)\sin\alpha_i - \rho_i \sin\left(\alpha_i - \dfrac{u_i}{\rho_i}\right) \\ 0 \\ \mp(\rho_i + a_i \cos\alpha_i)\cos\alpha_i \pm \rho_i \cos\left(\alpha_i - \dfrac{u_i}{\rho_i}\right) \end{bmatrix}. \tag{12}$$

Here, ρ_i is the radius of circular arc, and the upper sign corresponds to $i = 1$.

Representation of equations of the Blade in S_c

The coordinate transformation in transition from S_l via S_p to S_c is based on the following matrix equation

$$\mathbf{r}_c = [M_{cp}][M_{pl}]\mathbf{r}_l = [M_{cl}]\mathbf{r}_l\,. \tag{13}$$

The expressions for these matrices are given in the Appendix.

4. DERIVATION OF EQUATIONS OF GEAR TOOTH SURFACE

The gear tooth surface is generated in coordinate system S_2 by the head cutter blades as the head cutter rotates about the x_r-axis and the gear rotates about the gear axis with the unit vector $\mathbf{g}_2$ (Fig. 5).

The procedure of derivations is based on the following steps.

Step 1: *matrix representation of head cutter tilt*

Consider that initially coordinate system S_c for the untilted head cutter coincides with the coordinate system S_r that is located in plane $x_{c2} = 0$ and is rigidly connected to the cutting machine. To tilt the head cutter, it is turned through angle μ_2 about line m–m that is parallel to the y_r-axis (Fig. 10). Our goal is to represent the geometry of head cutter blades in coordinate system S_r taking into account that the head cutter has been turned about m–m and that it performs rotation about the x_r-axis.

Figure 11(a) shows coordinate systems S_c, S_p and S_l that are rigidly connected to the head cutter. Figure 11(b) shows an auxiliary coordinate system S_u whose axes y_u and x_u are parallel to the respective axes of S_c. Axes z_u and z_c coincide and the distance $O_c O_u = a$.

We consider also two rigidly connected coordinate systems S_n and S_m that are similar to S_c and S_u (Fig. 11b). Initially, before the tilt, S_m coincides with S_u, and S_n coincides with S_c, respectively. The tilt of the head cutter is performed about the y_m-axis (Fig. 11b). The product of matrices

$$[M_{nm}][M_{mu}][M_{uc}]\,[M_{cp}][M_{pl}] = [M_{nl}] \tag{14}$$

describes the coordinate transformation from S_l to S_n. For the particular case where $a = r_w$ the subproduct $[M_{uc}][M_{cp}]$ represents an identity matrix. For the case where $a \neq r_w$, the head cutter must be translated in the direction that is perpendicular to plane $x_m = 0$ to place point O_p in plane $x_m = 0$.

Step 2: *matrix representation of head cutter rotation*

We consider now that coordinate systems S_m, S_n and the head cutter are rigidly connected to each other. Initially, coordinate systems S_n and S_r coincide with each other. The head cutter and coordinate system S_n perform rotation about the x_r-axis and their orientation is shown in Fig. 12; ϕ_t represents the current angle of head cutter rotation.

Matrix $[M_{rn}]$ describes the rotation of the head cutter about the x_r-axis.

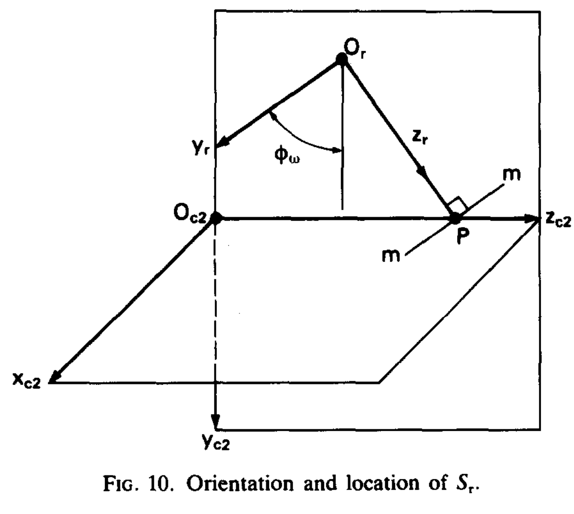

FIG. 10. Orientation and location of S_r.

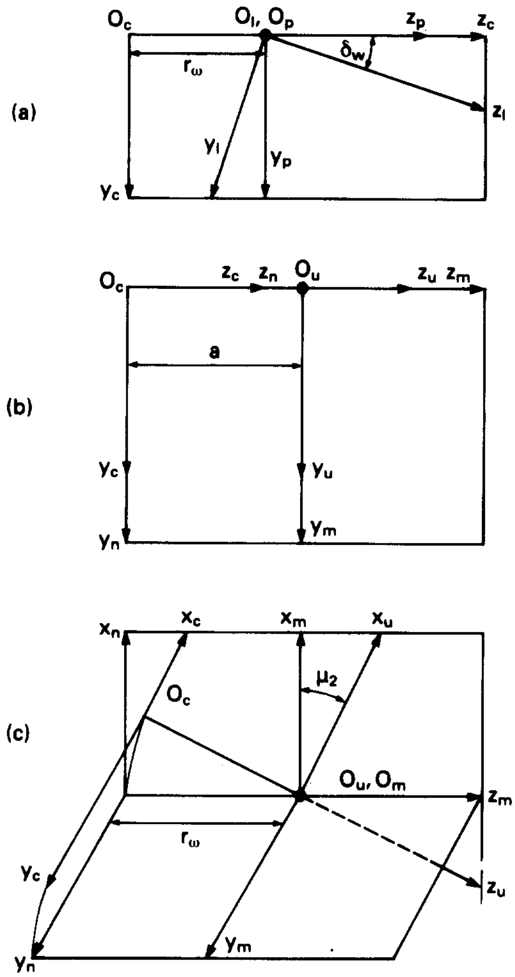

FIG. 11. Matrix representation of head cutter tilt.

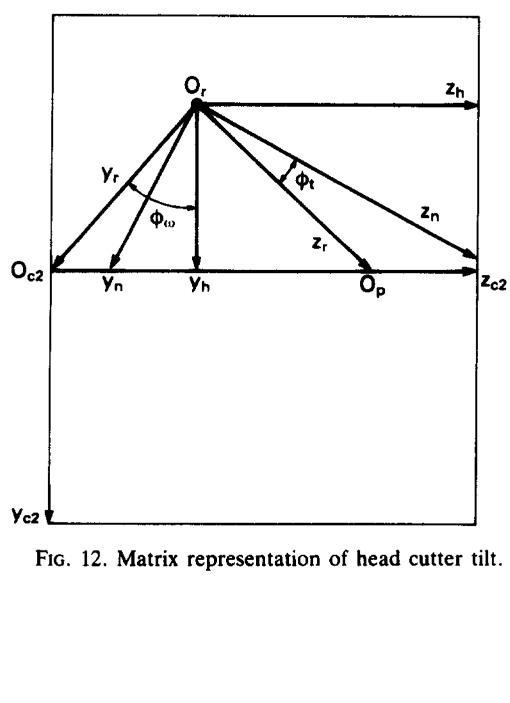

FIG. 12. Matrix representation of head cutter tilt.

Step 3: final expressions

To obtain the final equations of the gear tooth surface we use the following matrix equation

$$[r_2] = [M_{2d}][M_{dc_2}][M_{c_2h}]\,[M_{hr}][M_{rn}][M_{nm}]\,[M_{mu}][M_{uc}][M_{cp}][M_{pl}]\,[r_l(u_i)] \tag{15}$$

Matrix $[M_{c_2h}]$ describes the coordinate transformation from S_h to S_{c2} (Fig. 12). Matrices $[M_{dc_2}]$ describe the coordinate transformation from S_{c2} to S_d (Fig. 13) and $[M_{2d}]$ describes the rotation about the z_d-axis of the gear. Elements of matrix $[M_{rn}]$ and $[M_{2d}]$ are represented in terms of angles of rotation ϕ_t and ϕ_2 of the head cutter and the gear, respectively. However, these parameters are related since

$$\frac{\phi_t}{\phi_2} = \frac{N_2}{N_w} \tag{16}$$

and vector-function $\mathbf{r}_2(u_i, \phi_2)$ represents the gear tooth surface. Here: (u_i, ϕ_2) are the surface coordinates, where u_i (Fig. 9) represents the current parameter of the blade shape.

Normal $\mathbf{N}_2$ to surface Σ_2 is represented by the following vector equation:

$$\mathbf{N}_2 = \frac{\partial \mathbf{r}_2}{\partial u_i} \times \frac{\partial \mathbf{r}_2}{\partial \phi_2}. \tag{17}$$

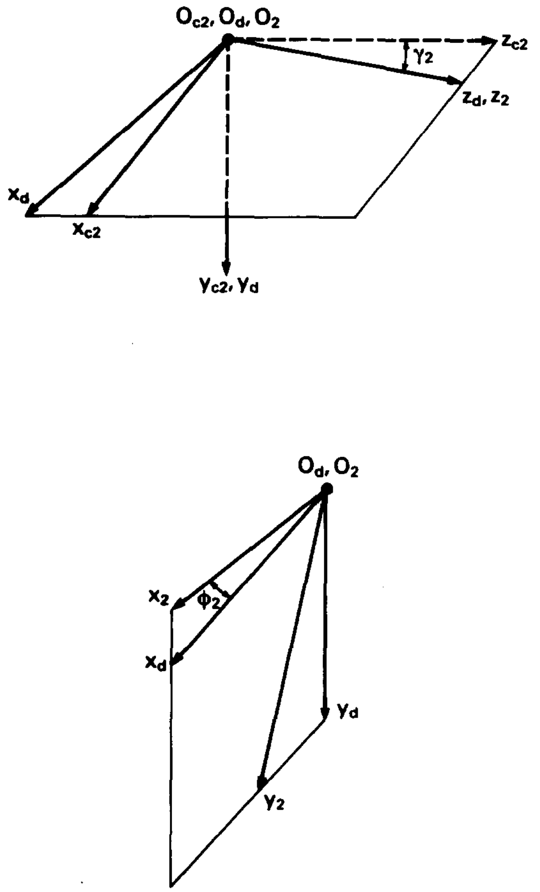

FIG. 13. Matrix representation of gear rotation.

Using equation (15) after differentiation, we obtain

$$\frac{\partial \mathbf{r}_2}{\partial u_i} = [L_{21}] \frac{\partial \mathbf{r}_e}{\partial u_i} \tag{18}$$

$$\frac{\partial \mathbf{r}_2}{\partial \phi_t} = \frac{\partial}{\partial \phi_2} [L_{2h}][L_{21}][\mathbf{r}_1^*(u)] \frac{\partial \phi_2}{\partial \phi_t} + [L_{2h}][L_{hr}] \left\{ \frac{\partial}{\partial \phi_t} [L_{rn}] \right\} [L_{n1}] \mathbf{r}_1^*(u_i) . \tag{19}$$

Matrix $[L]$ is a 3×3 sub-matrix of matrix $[M]$ that is obtained form $[M]$ by elimination of the fourth column and row; r_1^* is the 3×1 sub-column in $[r_1(u)]$.

To visualize the gear tooth surface a computer drawn 3-D image is represented in Fig. 14. Two sections of the surface are represented in Figs 15 and 16. One of these section (Fig. 15) is the mean cross-section of the gear that is perpendicular to the gear

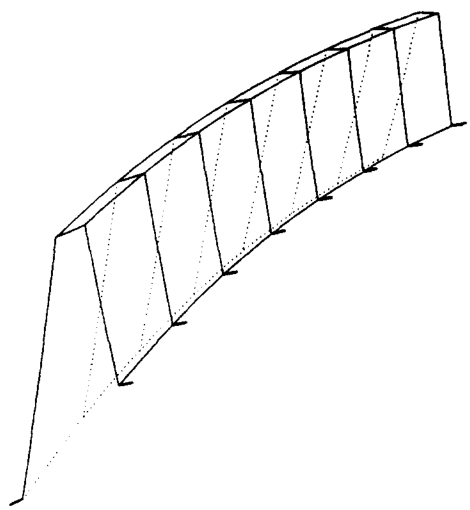

FIG. 14. 3-D Image of gear tooth surface.

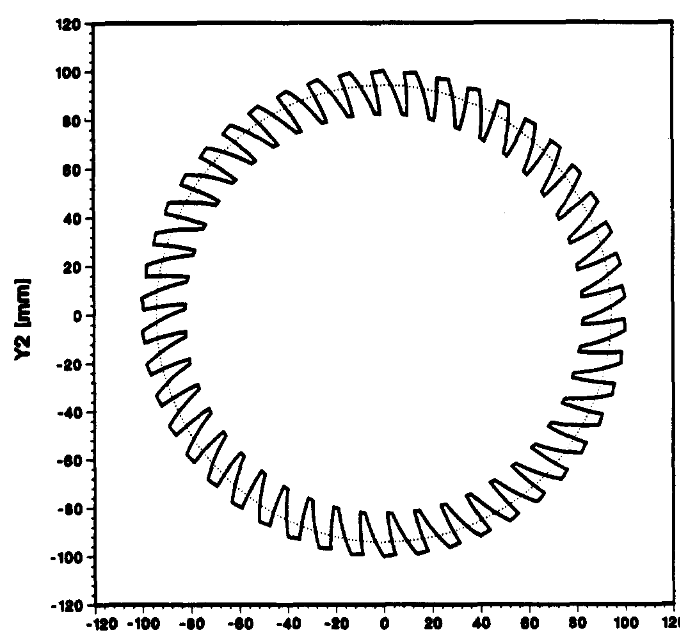

FIG. 15. Mean gear cross-section.

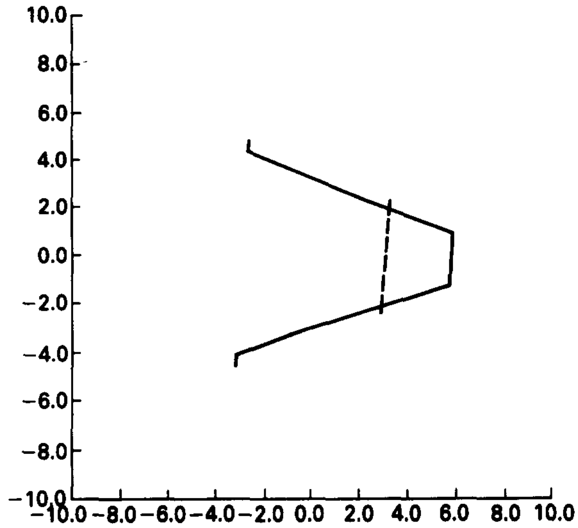

FIG. 16. Mean gear section (perpendicular to the generatrix of the pitch cone).

axis. The other one is obtained by cutting the surface by a plane that is perpendicular to the generatrix of the pitch cone.

These sections have been obtained for the gear with the following parameters:

Number of blade groups	N_w	11
Number of tooth	N_2	46
Head cutter radius	r_w	74 mm
Normal module	m_n	3.7190
Mean spiral angle	β_2	24.8133°
Pitch cone angle	γ_2	60.3370°
Mean cone radius	r_2	94.235 mm
Normal pressure angle (drive)	α_1	19.566°
Normal pressure angle (coast)	α_2	23.166°
Addendum		2.69 mm
Dedendum		5.87 mm
Angle for cutter tilt	μ_2	3.7456°
Curve blade radius	ρ	125 mm
Blade width	a_i	5.841 mm.

5. INSTALMENT PARAMETERS

The final expressions for the instalment of the head cutter are as follows:

The coordinates of point O_r (Fig. 11) are represented by

$$\overline{O_{c2}O_r} = \begin{bmatrix} 0 \\ -V \\ H \end{bmatrix} = \begin{bmatrix} 0 \\ -r_w \cos(\beta_2 - \delta_w) \\ \dfrac{r_2}{\sin\gamma_2} - r_w \sin(\beta_2 - \delta_w) \end{bmatrix}. \tag{20}$$

The orientation of O_rO_p is determined with the swivel angle ϕ_w (Fig. 5) that is represented by equation (5). The initial orientation of the head cutter axis is represented in S_{c2} by the unit vector

$$\mathbf{c} = [\cos\mu_2 \quad \sin\mu_2 \sin\phi_w \quad \sin\mu_2 \cos\phi_w]^T. \tag{21}$$

6. CONCLUSIONS

(1) The concept and the kinematics for the process of generation of the member-gear of a hypoid gear drive have been described (see Sections 1 and 2).

(2) The geometry of the applied tool has been discussed (Section 3).

(3) Equations of the generated gear tooth surface for its representation in 3-D space have been derived (Section 4). These equations are necessary for: (i) generation of dies if the gear is forged, (ii) minimization of irregularities of gear tooth surface by correction of machine-tool settings, and (iii) computerized simulation of meshing and contact for a hypoid gear drive. A computer drawn 3-D image and sections of gear tooth surface have been represented (Section 4).

REFERENCES

[1] Gleason Works, Understanding tooth contact analysis, Rochester, NY 14692, Publication No. SD3139 (1981).
[2] F. L. LITVIN and Y. GUTMAN, Methods of synthesis and analysis for hypoid gear drives of "Formate" and "Helixform", Parts 1–3, *ASME J. Mech. Des.* **103**, 83–113 (January 1981).
[3] F. L. LITVIN, Theory of gearing, NASA publication; 1212 (AVSCOM technical report; 88-c-035) (1989).
[4] R. O. CHAMBERS and R. E. BROWN, Coordinate measurement of bevel gear teeth, SAE Int. Off-Highway and Powerplant Congress (1987).
[5] Gleason Works, G.-Age T.M. user's manual for the Gleason automated gear evaluation system used with Zeiss coordinate measuring machines (1987).
[6] Gleason Works, Tooth contact analysis, formulas & calculation procedure, Rochester, NY 14692, Publication No. SD3115 (1964).
[7] F. L. LITVIN, Y. ZHANG, J. KIEFFER and R. F. HANDSCHUH, Identification and minimization of deviations of real gear tooth surfaces, *ASME J. Mech. Des.* (in press).
[8] A. SHABANA, *Dynamics of Multibody Systems*. Wiley, New York (1989).

APPENDIX: EXPRESSIONS FOR DERIVED MATRICES

Matrix $[M_{pl}]$ is represented by

$$[M_{pl}] = \begin{bmatrix} 1 & 0 & 0 & 0 \\ 0 & \cos\delta_w & \sin\delta_w & 0 \\ 0 & -\sin\delta_w & \cos\delta_w & 0 \\ 0 & 0 & 0 & 1 \end{bmatrix}. \tag{A1}$$

Matrix $[M_{cp}]$ is represented by

$$[M_{cp}] = \begin{bmatrix} 1 & 0 & 0 & 0 \\ 0 & 1 & 0 & 0 \\ 0 & 0 & 1 & r_w \\ 0 & 0 & 0 & 1 \end{bmatrix}. \tag{A2}$$

Matrix $[M_{uc}]$ is represented by

$$[M_{uc}] = \begin{bmatrix} 1 & 0 & 0 & 0 \\ 0 & 1 & 0 & 0 \\ 0 & 0 & 1 & -a \\ 0 & 0 & 0 & 1 \end{bmatrix}. \tag{A3}$$

Matrix $[M_{mu}]$ is represented by

$$[M_{mu}] = \begin{bmatrix} \cos\mu_2 & 0 & -\sin\mu_2 & 0 \\ 0 & 1 & 0 & 0 \\ \sin\mu_2 & 0 & \cos\mu_2 & 0 \\ 0 & 0 & 0 & 1 \end{bmatrix}. \tag{A4}$$

Matrix $[M_{\mathrm{nm}}]$ is represented by

$$[M_{\mathrm{nm}}] = \begin{bmatrix} 1 & 0 & 0 & 0 \\ 0 & 1 & 0 & 0 \\ 0 & 0 & 1 & r_{\mathrm{w}} \\ 0 & 0 & 0 & 1 \end{bmatrix}. \tag{A5}$$

Matrix $[M_{r\mathrm{n}}]$ is represented by

$$[M_{r\mathrm{n}}] = \begin{bmatrix} 1 & 0 & 0 & 0 \\ 0 & \cos\phi_{\mathrm{t}} & -\sin\phi_{\mathrm{t}} & 0 \\ 0 & \sin\phi_{\mathrm{t}} & \cos\phi_{\mathrm{t}} & 0 \\ 0 & 0 & 0 & 1 \end{bmatrix}. \tag{A6}$$

Matrix $[M_{\mathrm{h}r}]$ is represented by

$$[M_{\mathrm{h}r}] = \begin{bmatrix} 1 & 0 & 0 & 0 \\ 0 & \cos\phi_{\mathrm{w}} & \sin\phi_{\mathrm{w}} & 0 \\ 0 & -\sin\phi_{\mathrm{w}} & \cos\phi_{\mathrm{w}} & 0 \\ 0 & 0 & 0 & 1 \end{bmatrix}. \tag{A7}$$

Matrix $[M_{\mathrm{c_2h}}]$ is represented by

$$[M_{\mathrm{c_2h}}] = \begin{bmatrix} 1 & 0 & 0 & 0 \\ 0 & 1 & 0 & -V \\ 0 & 0 & 1 & H \\ 0 & 0 & 0 & 1 \end{bmatrix}. \tag{A8}$$

Matrix $[M_{\mathrm{dc_2}}]$ is represented by

$$[M_{\mathrm{dc_2}}] = \begin{bmatrix} \cos\gamma_2 & 0 & -\sin\gamma_2 & 0 \\ 0 & 1 & 0 & 0 \\ \sin\gamma_2 & 0 & \cos\gamma_2 & 0 \\ 0 & 0 & 0 & 1 \end{bmatrix}. \tag{A9}$$

Matrix $[M_{\mathrm{2d}}]$ is represented by

$$[M_{\mathrm{2d}}] = \begin{bmatrix} \cos\phi_2 & -\sin\phi_2 & 0 & 0 \\ \sin\phi_2 & \cos\phi_2 & 0 & 0 \\ 0 & 0 & 1 & 0 \\ 0 & 0 & 0 & 1 \end{bmatrix}. \tag{A10}$$